

Experimental study of the Be–Si phase diagram

ZHU PAN, YONG DU, BAIYUN HUANG, HONGHUI XU, YONG LIU*, HAILIN CHEN, WEI XIONG
State Key Laboratory of Powder Metallurgy, Central South University, Changsha, Hunan 410083,
People's Republic of China
E-mail: yong-du@mail.csu.edu.cn

R. SCHMID-FETZER
Institute of Metallurgy, TU Clausthal, Robert-Koch Strasse 42, D-38678, Clausthal-Zellerfeld, Germany

Published online: 3 February 2006

Wang *et al.* [1] reported that minor addition of Be in the as-cast Al-11Si-0.3Mg alloy (wt.%) causes faster precipitation and more heat effect of metastable β' than the alloy without addition of Be and considerably increases the peak hardness achieved during as-cast aging. Both Yin *et al.* [2] and Yie *et al.* [3] have found that the addition of Be into commercial Al alloys, such as Al-4.93Si-1.4Fe-0.63Mg-1.45Cu [2] and Al-11.1Si-1.03Fe-0.08Ti alloys [3], is beneficial for the transformation of the needle-shaped iron-rich phase into the Chinese scripts. It is generally believed that the needle-shaped iron-rich phase is harmful to the strength and ductility of materials. The influence of Be addition on the quasicrystal-forming ability in Al-based alloys, such as alloys in the Al–Cu–Fe and Al–Mn systems, has been investigated [4]. It was found that Be addition modified the icosahedral phase (i-phase) formation mechanism from peritectic reaction to primary solidification and resulted in the increase of the volume fraction for the i-phase [4]. In addition, the substitution of Al by Be was found to reduce significantly the critical Mn content and cooling rate necessary for the formation of i-phase [4]. Chen *et al.* [5] demonstrated that the partial substitution of Al by Si in Al₈₀Mn₂₀ (at.%) binary alloy completely suppresses the formation of a pentagonal quasicrystalline T-phase and drastically modifies the microstructure of the i-phase. Consequently, knowledge of the phase diagram and thermodynamic properties in the Be–Si system is of fundamental importance for guiding the design and processing of Al-based quasi-crystal materials and multi-component commercial Al alloys.

The phase relationship in the Be–Si system has been subjected to several investigations [6–10]. This binary phase diagram was shown to be a simple eutectic one. Masing and Dahl [6] are responsible for the major contribution to the establishment of the Be–Si phase diagram. By means of thermal analysis technique, they [6] measured the phase transition temperatures for four bi-

nary alloys with starting materials of purity 99% Be and 99.95% Si. The eutectic point was determined to be 1090 °C and 33.42 at.% Si [6]. Following the same method, Gelles and Pickett [7] measured the phase transition temperatures for two binary Be-rich alloys (0.5 and 2.5 at.% Si). According to the thermal effect signals on heating [7], the eutectic temperature is 1073 ± 8 °C. The mutual solid solubilities between Be and Si were investigated by several groups of authors [8–10]. Using X-ray diffraction (XRD) technique, Sloman [8] reported that there is nearly no solid solubility of Si in Be. Employing XRD and metallographic methods, Hindle and Slattery [9] found that the solid solubility of Be in (Si) is less than 0.008 at.%. Using electron probe microanalysis (EPMA) technique, Kleykamp [10] recently reported that the solubility of Si in (Be) at 690 °C is 0.006 at.% Si, confirming the previous findings [8]. Based on mainly the experimental data published in 1929 and the limited experimental data [7], Okamoto and Tanner [11] assessed the eutectic point to be at 1090 ± 10 °C and 36 ± 3 at.% Si. In the binary phase diagrams compiled by Massalski [12], the Be–Si phase diagram is redrawn from the one assessed by Hansen and Anderko [13]. The present work aims at establishing an accurate Be–Si phase diagram by means of XRD, differential thermal analysis (DTA) methods, supplemented by microstructure observations.

The starting materials used in the present work are 99.8% purity Be pieces (Northwest Institute for Non-ferrous Metal Research, Xi'an, China) and 99.9999% purity Si pieces (Johnson Matthey Company, MA 01835, USA). In addition to pure Be and Si, six binary alloys with the weight of about 1.5 g were prepared by arc melting Be and Si pieces under 99.99% purity argon atmosphere. Table I lists the compositions of the alloys. No chemical analysis for the alloys was performed since the weight losses during arc-melting were generally less than 1 mass%. The as-cast alloys were sealed in evacuated silica tubes under vacuum of 10^{-3} bar, and annealed at

* Author to whom all correspondence should be addressed.

TABLE I Summary of the phases for the samples in the Be–Si system annealed at 1050 °C for 7 days, and phase transition temperatures measured subsequently by DTA

No	at.% Si	Phase ^a	Transition temperature (°C) ^b
1	0	(Be)	1251, 1285
2	10	(Be)+(Si)	1086, 1381
3	20	(Be)+(Si)	1085, 1347
4	50	(Be)+(Si)	1085, 1300
5	70	(Be)+(Si)	1084, 1206
6	80	(Be)+(Si)	1085, 1163
7	90	(Be)+(Si)	1085, 1204
8	100	(Si)	1414

^aThe phase is identified with XRD, metallography, and SEM/EDX methods.

^bObtained on heating with a heating rate of 5 K/min.

1050 ± 1 °C for 7 days, and then water-quenched. Heat treatment was performed by using a high-temperature diffusion furnace (type L-45-1-135, QingDao, China).

A high-temperature DTA apparatus (STA 409 PC, Netzsch, Germany) was used to measure phase transition temperatures. Both the sample holder and reference material are Al₂O₃. Solid pieces with weights of about 40–80 mg were taken from the annealed samples. The measurement was carried out between room temperature and 1450 °C with a heating and cooling rate of 5 K/min in argon atmosphere. The temperature was measured with Pt–Pt/Rh thermocouples and calibrated to the melting temperatures of Al (660.32 °C), Au (1064.18 °C), and Si (1413.85 °C). The accuracy of the temperature measurement was estimated to be ± 2 °C. The onset of the first DTA peak corresponds to the invariant reaction temperature, and the liquidus temperature is taken to be the peak maximum of the second DTA peak. The phase transition tempera-

tures were taken from the heating curves since reactions between samples and Al₂O₃ crucible material could not be completely excluded and supercooling phenomenon usually accompanies solidification.

The phase identification was made by means of XRD (Rigaku D/max2550VB, Japan) using Cu K α ₁ radiation with Ge as an internal standard. Lattice parameters were calculated by using the program JADE [14].

The microstructure observation was performed with optical microscopy (Leica DMLP, Wetzlar, Germany) and scanning electron microscopy (SEM) (JSM-5600LV, Japan Electron Optics Laboratory, Japan) with energy dispersive X-ray analysis (EDX).

Table I summarizes the phases identified by XRD, optical microscopy, and SEM/EDX techniques along with the phase transition temperatures resulting from DTA measurements. The lattice parameters of (α Be) and (Si) calculated from the binary alloys match closely those for the pure elements [15]. Thus, binary solubilities in these phases are presumably negligible. This confirms the previous findings [8–10].

The back scattering images for representative samples (60 at.% Si and 80 at.% Si) are presented in Figs. 1 and 2, respectively. As shown in Fig. 1, the alloy Be_{0.4}Si_{0.6} in as-cast state shows the existence of a eutectic structure and primary (Si) phase. Fig. 2 clearly indicates the (α Be) and (Si) phases for the alloy Be_{0.2}Si_{0.8} annealed at 1050 °C for 7 days.

In these excellently reproducible measurements, the general features of the previously established Be–Si phase diagram [6–10] are confirmed. However, the quantitative data need to be revised and an amendment of the phase diagram published in recent handbooks [11, 12] is necessary.

Based on the experimental data mainly from the present work, the revised Be–Si phase diagram is presented in

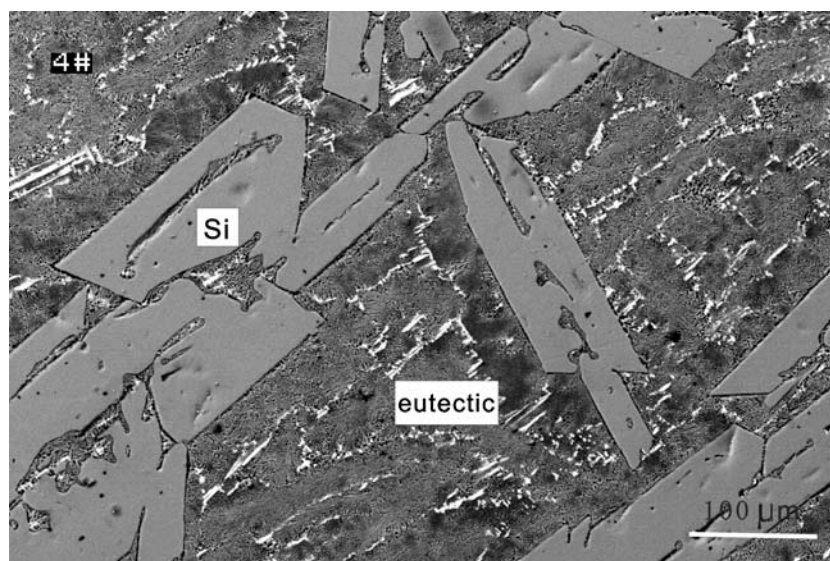


Figure 1 Back scattering image of as-cast Be_{0.4}Si_{0.6} (atomic fraction) alloy.

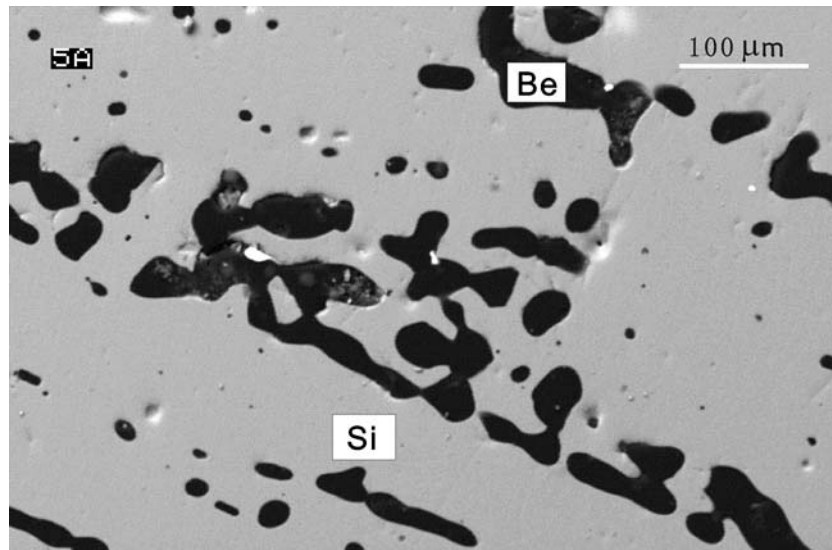


Figure 2 Back scattering image of $\text{Be}_{0.2}\text{Si}_{0.8}$ (atomic fraction) alloy annealed at $1050\text{ }^{\circ}\text{C}$ for 7 days.

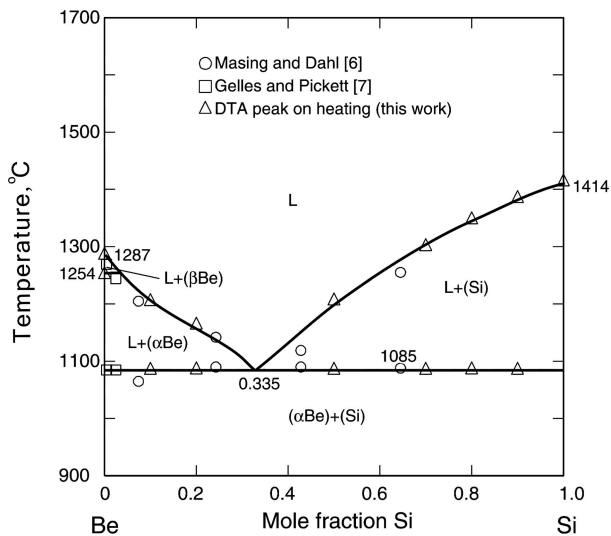


Figure 3 Revised Be–Si phase diagram compared with the experimental data of present and previous studies. The mutual solid solubilities were found to be below the XRD detection limit in agreement with the reported 0.006 at.% Si in (Be) at $690\text{ }^{\circ}\text{C}$ [8,10] and a limit of less than 0.008 at.% Be in (Si) [9].

Fig. 3 along with the literature values. In view of the virtually zero solubility of Si in (Be), the invariant reaction among liquid, (αBe), and (βBe) is assumed to be of degenerated feature: (αBe) = (βBe), L at $1254\text{ }^{\circ}\text{C}$.

The eutectic point is located at $1085 \pm 2\text{ }^{\circ}\text{C}$ and 33.5 at.% Si. This eutectic point agrees reasonably with the previously accepted value, $1090\text{ }^{\circ}\text{C}$ and 36 ± 3 at.% Si [11], but for the liquidus line noticeable discrepancies are observed for the present results and the earlier data [6]. The present experimental results are considered preferable on the grounds that (I) high purity of starting materials are used and the metal pieces have been burnished in order to remove oxide from the surface, (II) the samples are annealed at $1050\text{ }^{\circ}\text{C}$ for 7 days, just below

the eutectic temperature in order to reach equilibrium, and (III) the experimental results from different experimental methods are consistent with each other.

The presently obtained Be–Si phase diagram is expected to substitute for the currently accepted version [11, 12].

Acknowledgments

This research work is supported by National Outstanding Youth Science Foundation of China through grant No.50425103 and National Advanced Materials Committee of China through grant No. 2003AA302520. Y. Du gratefully acknowledges the Furong Chair Professorship program released by Hunan province of P.R. China for financial support. The donation of Leica DMLP microscope from Alexander von Humboldt foundation is greatly appreciated.

References

1. G. Q. WANG, X. F. BIAN and J. Y. ZHANG, *Acta Metall.* **39** (2003) 43.
2. F. YIN, J. B. YANG, Y. X. WANG and G. X. WANG, *Foundry* **49** (2000) 829.
3. S. N. YIE, S. L. LEE, Y. H. LIN and J. C. LIN, *Mater. Trans. JIM* **40** (1999) 294.
4. G. S. SONG, E. FLEURY, S. H. KIM, W. T. KIM and D. H. KIM, *J. Alloys Compd.* **342** (2002) 251.
5. S. H. CHEN, D. KOSKENMAKI and C. H. CHEN, *Phys. Rev. B* **35** (1987) 3715.
6. G. MASING and O. DAHL, *Wiss. Veroff. Siemens-Konzern* **8** (1929) 248.
7. S. H. GELLES and J. J. PICKETT, *At. Energy Commun. NMI-1218* (1960) 44.
8. H. A. SLOMAN, *J. Inst. Met.* **49** (1932) 365.
9. E. D. HINDLE and G. F. SLATTERY, *ibid.* **28** (1963) 651.
10. H. KLEYKAMP, *J. Nucl. Mater.* **294** (2001) 88.
11. H. OKAMOTO and L. E. TANNER, in "Phase Diagrams of Binary Beryllium Alloys" (ASM, Metals Park, OH, 1987) p. 186.

12. T. B. MASSALSKI, in "Binary Alloys Phase Diagrams" (ASM, Metals Park, OH, 1986) p. 475.
13. M. HANSEN and K. ANDERKO, in "Constitution of Binary Alloys" (McGraw-Hill, New York, 1958).
14. "JADE, User's Guide for XRD Pattern Processing", (Materials Data, Livermore, CA) (2001).
15. P. VILLARS and L. D. CALVERT, in "Pearson's Handbook of Crystallographic Data for Intermetallic Phases" (ASM International, Materials Park, OH, 1991).

*Received 30 July 2004
and accepted 25 May 2005*